

Mechanisms associated with progression from lobar inflammation to bilateral lung injury: an experimental study

Received: 1 November 2025

Accepted: 25 January 2026

Published online: 02 February 2026

Cite this article as: Mauri T., Spinelli E., Marongiu I. *et al.* Mechanisms associated with progression from lobar inflammation to bilateral lung injury: an experimental study. *Respir Res* (2026). <https://doi.org/10.1186/s12931-026-03546-0>

Tommaso Mauri, Elena Spinelli, Ines Marongiu, Anna Damia, Marco Leali, Alice Maretti, Leonardo Consalvo, Francesco Damarco, Gianluca Lopez, Alberto Zanella, Lorenzo Rosso, Valentina Vaira & Giacomo Grasselli

We are providing an unedited version of this manuscript to give early access to its findings. Before final publication, the manuscript will undergo further editing. Please note there may be errors present which affect the content, and all legal disclaimers apply.

If this paper is publishing under a Transparent Peer Review model then Peer Review reports will publish with the final article.

Mechanisms associated with progression from lobar inflammation to bilateral lung injury: an experimental study

Tommaso Mauri^{1,2,*}, Elena Spinelli^{1,*}, Ines Marongiu¹, Anna Damia², Marco Leali², Alice Maretti², Leonardo Consalvo², Francesco Damarco³, Gianluca Lopez^{4,5}, Alberto Zanella^{1,2}, Lorenzo Rosso³, Valentina Vaira^{4,5}, Giacomo Grasselli^{1,2}

1. Department of Anesthesia, Critical Care and Emergency, Fondazione IRCCS Ca' Granda Ospedale Maggiore Policlinico, Milan, Italy
2. Department of Pathophysiology and Transplantation, University of Milan, Italy
3. Division of Thoracic Surgery and Lung Transplantation, Fondazione IRCCS Ca' Granda Ospedale Maggiore Policlinico, Milan, Italy.
4. Division of Pathology, Fondazione IRCCS Ca' Granda Ospedale Maggiore Policlinico, Milan, Italy.
5. Department of Biomedical Surgical and Dental Sciences, University of Milan, Milan, Italy.

* co-first authors

Corresponding Author:

Tommaso Mauri

Department of Pathophysiology and Transplantation, University of Milan

Via F. Sforza 35, 20122 Milan, Italy

E-mail: tommaso.mauri@unimi.it

Abstract

Background: Localized lung insult, such as pneumonia, can increase respiratory drive and effort. The interplay between the initial injury, the inflammatory reaction and increased drive and effort could damage other areas and progress to bilateral lung injury.

We aimed to describe the pathophysiological mechanisms causing injury in previously healthy regions of contralateral lung, when respiratory drive and effort were increased by lobar inflammation.

Methods: Localized pulmonary inflammation was induced through instillation of 0.5 mg/kg lipopolysaccharide (LPS) in the left lower lobe of 18 pigs, while 5 animals served as sham controls. After 24 hours of spontaneous breathing, the severity of right lung injury was assessed by the validated histological score and correlated with potential physiological and biological determinants.

Results: Animals challenged with lobar inflammation developed bilateral lung injury, associated with increased respiratory drive and effort.

Histological score of the right lung was characterized by wide inter-individual variability (median 11 [8-14], range 3-25). Right lung injury score was correlated with respiratory drive and effort; with respiratory rate and minute ventilation, but not with tidal volume; with peak inspiratory and driving transpulmonary pressures, and with EIT-derived lung strain; with lower sub-atmospheric alveolar pressure and with more negative end-expiratory transpulmonary pressure.

Right lung injury score was also correlated with inflammatory plasma cytokines: higher SDF-1 α and lower IL-1Ra, IL-5 and GM-CSF.

Conclusions: An experimental model of localized lung inflammation allowed us to investigate the role of specific pathophysiological mechanisms for the development of injury in previously healthy lung regions.

Keywords: respiratory effort; self-inflicted lung injury; inflammation; spontaneous breathing

ARTICLE IN PRESS

Introduction

Progression from local insult (e.g., pneumonia or contusion) to bilateral lung injury could result from multiple pathophysiological mechanisms, triggered by elevated inspiratory drive and effort (1). Increased spontaneous respiratory activity has been associated with worsening bilateral lung injury, (2–5) while studies on its role in the progression from local to bilateral injury lack. In patients with the acute respiratory distress syndrome (ARDS), the association between increased respiratory effort, worsening injury and poor outcomes is supported by recent pilot studies (3, 6–12). In milder bilateral lung injury, instead, spontaneous breathing could protect the lung, likely because of lower inspiratory effort and less susceptibility (3, 13). Studies focused on the development of injury in previously healthy lung regions, with a longer observation period and comprehensive assessment of its pathophysiological mechanisms are scant, if any. An early pivotal experimental study showed that hyperventilation could induce injury in healthy lungs (14). However, respiratory drive was increased by acidification of the cerebrospinal fluid, which may not translate to patients with pneumonia, in whom localized pulmonary injury, inflammation and respiratory effort likely act synergistically in the progression to diffuse injury.

Both self-inflicted lung injury (SILI) and ventilation-induced lung injury (VILI) are caused by excessive mechanical stress and strain, but with some differences. Large drops in pleural pressure generated by strong inspiratory efforts are uneven, with risk of regional injury due to high local transpulmonary pressures and focal alveolar overdistension exacerbated by gas shift within the lungs (pendelluft). They also facilitate pulmonary edema formation through increased pulmonary capillary hydrostatic pressure and transvascular pressure gradient.

In the present study, we reasoned that understanding mechanisms involved in the progression from localized inflammation to bilateral lung injury (i.e., as in clinical evolution from pneumonia to ARDS) could have both pathophysiological and clinical significance, given the

association between worsening lung injury, the risk for intubation and mortality (9, 15). We developed an experimental model of localized pulmonary inflammation induced through the instillation of lipopolysaccharide (LPS) in the left lower lobe of healthy swine. The main endpoint was the description of mechanisms leading to the development of injury at 24 hours in the initially healthy right lung. Briefly, we described the development of right lung injury, but with large variability in terms of severity. Then, we investigated the correlation between the severity of right lung injury and candidate pathophysiological mechanisms, including increased respiratory drive and effort, lung stress and strain, alveolar and transpulmonary pressure and pendelluft measured by advanced respiratory monitoring, such as esophageal pressure (Pes) and electrical impedance tomography (EIT). Third, we explored the correlation of plasma proteomics profile with the severity of right lung injury and with effort.

Methods

This experimental study in a porcine model was approved by the Italian Ministry of Health, Rome, Italy (Ref. n° 855/2024-PR prot. 568EB.49) and conducted according to the European Directive 2010/63/EU on the protection of animals used for scientific studies and the Italian decree 26/2014.

Animal preparation. Healthy female pigs were anesthetized, tracheostomized and instrumented with pulmonary artery and carotid artery catheters to monitor hemodynamics and collect blood samples. An EIT monitoring belt (PulmoVista 500; Drager, Lubeck, Germany) was placed around the thorax and Pes catheter was inserted and calibrated. See the Online Supplement for further details.

Study protocol. Eighteen deeply sedated pigs lying on the left side and on controlled ventilation (LPS group) underwent bronchoscopic instillation of 0.5 mg/kg of E. coli LPS

(LPS 055:B5; Product no. L2880; Sigma Aldrich, Saint Louis, MO) into the inferior lobe of the left lung. Bronchoscopy was performed by experienced thoracic surgeon. Five pigs underwent the same protocol (preparation, anesthesia, instrumentation and management) but did not receive LPS (Sham group).

Then, animals were positioned prone, and sedation was decreased to the minimal propofol dose useful to maintain autonomous respiratory drive, without excessive movements for safety reasons. The experiment started upon start of spontaneous breathing (pressure support ventilation with PEEP 5 cmH₂O, support 5 cmH₂O, FiO₂ 0.5) and lasted for 24 hours.

At the end of the experiment, blood samples were collected and processed for plasma proteomics (see below). Three lung tissue samples from each lung were taken for histological analysis and immunohistochemistry. Severity of lung injury was then quantified by validated lung histological score (16) performed by a blinded pathologist.

Measurements. Measurements were performed after 6 and 12 hours after start of the experiment, as well as the end. A 5-minute continuous recording of airway, esophageal and transpulmonary pressure waveforms including short end-inspiratory and end expiratory occlusions was collected, synchronized with EIT ventilation data. Data were analyzed offline to obtain average values of: respiratory rate (RR), tidal volume (V_t) and minute ventilation (MV); airway occlusion pressure (P_{0.1}), esophageal pressure swing (ΔP_{es}), airway pressure deflection (ΔP_{occ}); transpulmonary driving pressure ($\Delta P_L = [P_{plat} - P_{eS_{end-insp}}] - [PEEP - P_{eS_{end-exp}}]$); dynamic end-inspiratory transpulmonary pressure ($P_{L_{insp}}$); Pressure-Time Product (PTP, calculated as the time integral of the difference between P_{es} and the static recoil pressure of the chest wall during inspiration, given that P_{es} reflects the difference between muscular pressure, P_{mus} , and elastic recoil pressure of the chest wall (17)), both per minute (PTP_{min}) and per breath (PTP_{breath}).

From offline analysis of EIT data we obtained: global and regional ventilation (18), tidal deformation of the lung (a surrogate for lung strain) (19), and occult pendelluft (20), as previously described. Alveolar pressures were estimated by recursive least square fitting of transpulmonary pressure and EIT data (21).

Systemic and pulmonary hemodynamics, arterial and mixed venous blood gas analyses, diuresis, fluid balance and dose of sedative drugs were also collected.

At the end of the experiment, plasmatic levels of 105 inflammatory mediators were evaluated with the Human XL Cytokine Array Kit (R&D system, Minneapolis, MN USA).

See the online supplement for details on physiologic and EIT measurements, histology and proteomic analyses.

Statistical analysis. Variables are presented as mean and SD or median and interquartile range [IQR], according to their distribution, as assessed using the Shapiro-Wilk test. Comparisons of continuous data between groups were done using one-way ANOVA, if performed only at one time point, or mixed ANOVA for repeated measures to assess the effect of time. Univariate linear mixed-effect model was performed for each candidate physiological and biological variable with the right lung injury histological score as the dependent variable. Linearity, homoscedasticity and normality of residuals were tested for all models. Correlation coefficients (r) and associated p -values were calculated. Statistical analysis was conducted with JMP® Pro software, Version 16 (SAS Institute Inc., Cary, NC) and results were considered statistically significant at $p < 0.05$.

Results

Development of bilateral lung injury. Instillation of LPS in the left lower lobe, followed by 24 hours of spontaneous breathing, resulted in the development of bilateral lung injury in the

LPS group compared to Sham. Table 1 shows the main pathophysiological differences between study groups: in the LPS group, histological lung injury was bilateral, with mild deterioration in gas exchange and more relevant impairment of respiratory mechanics. In comparison to Sham, respiratory drive and effort, lung stress and minute ventilation were increased in the LPS group, with equal dose of sedative drugs. Lower PaCO₂ indicated more activated respiratory drive, too. Hemodynamics were stable and comparable in both groups (apart from higher heart rate due to inflammation and higher work of breathing), as well as fluid balance (Table 1).

Histopathological characteristics of right lung injury. Figure 1 shows the variability in the severity of right lung injury: the histological score assessed by blinded pathologist and extensively validated showed a normal distribution (Shapiro-Wilk $p = 0.27$) across a wide range of values (3 to 25). Of note, within the relatively short observation period (24 hours), 50% of the animals already developed moderate-severe right lung injury based on previous publications (i.e., histological injury score of the right lung >10).

Figure 2 shows representative histological images of right lung SILI, with two degrees of severity (right lung injury score ≤ 10 for milder vs. > 10 for more severe), compared to Sham. Mild alveolar epithelial injury with granulocyte infiltration characterized less severe right lung injury (Figure 2b), while alveolar disruption and massive exudate altered the lung structure in more severe right injury (Figure 2a). Immunohistochemistry assay showed progressive abundance of macrophages, with aggregation in clusters in more severe right lung injury (Figure 2d and 2e).

Pathophysiological mechanisms of progression to right lung injury. In terms of ventilatory pattern, we observed correlations between right histological score, respiratory rate ($r = 0.47$, $p = 0.048$) and minute ventilation ($r = 0.56$, $p = 0.016$), but not with inspired tidal volume ($r = 0.16$, $p = 0.54$) (Figure 3a-c). When we analyzed inspiratory drive and effort, right lung injury

score was correlated with $P_{0.1}$ ($r = 0.54$ $p = 0.021$), ΔP_{occ} ($r = 0.63$ $p = 0.005$) and ΔP_{es} ($r = 0.74$ $p < 0.001$) (Figure 4a-c). The metabolic work of breathing per minute (PTPmin) was correlated to higher histological score ($r = 0.72$ $p = 0.007$), too, likely indicating a potential additional role for respiratory rate (Figure 3d). The right lung injury score was also correlated with lower value of alveolar pressure (P_{alv}) measured during inspiration ($r = -0.48$ $p = 0.042$), which increases stretch of the alveolar wall cells and the risk for fluids extravasation (Supplemental Figure 1a). Indeed, P_{alv} ranged from -3 to + 4 cmH₂O, reaching sub-atmospheric values in animals with more severe right lung involvement.

Higher right lung injury score was correlated with inspiratory mechanical lung stress and strain (Figure 5a-b). Dynamic inspiratory transpulmonary pressure (P_{Linsp}) and driving transpulmonary pressure (ΔP_L) (i.e., the main measures of inspiratory stress) were correlated with its severity ($r = 0.54$ $p = 0.019$ and $r = 0.74$ $p < 0.001$, respectively). In addition, tidal deformation of the right lung (i.e., the regional lung strain measured by EIT, see Figure 2 g-i) was strongly correlated with the right injury score ($r = 0.88$ $p < 0.001$), too (Figure 5c).

Animals ventilated with PEEP values lower than P_{es} end-exp (i.e. negative values of $P_{Lend-exp}$, reflecting higher risk of alveolar collapse) developed more severe right lung injury ($r = -0.59$ $p = 0.009$) (Supplemental Figure 1b).

At variance from previous works (4), we did not observe an association between occult pendelluft during inspiration and right lung injury score ($r = 0.36$ $p = 0.138$) (Fig 5d), possibly indicating a difference in the injurious mechanisms involved in progression from lobar insult to bilateral injury as compared to those involved in worsening of severe ARDS. Hemodynamics, both central and systemic, were not correlated with the right lung injury score (Online Supplement Table E1). Finally, in contrast with recent data (17), fluid balance was not correlated with the progression of injury ($r = -0.09$ $p = 0.729$).

Time-course of pathophysiological mechanisms of progression to bilateral injury. We compared the relevant variables in animals developing milder vs. more severe right lung injury (median value of right lung SILI score ≤ 10 vs. > 10) at T6 and T12. The respiratory drive and effort parameters, P0.1, ΔP_{es} and driving transpulmonary pressure started to separate at 12 hours (Online Supplemental Table E2 and Figure 2). These data could support clinical observations that worsening respiratory failure in spontaneously breathing patients is best predicted at 12 hours (18). Indeed, the correlation between ΔP_{es} and right lung injury was significant already at 12 hours ($r = 0.85$ $p < 0.001$).

Plasma proteomics and development of right lung injury. The correlation between the circulating levels of inflammatory mediators and the right lung injury score was explored by proteomic approach (Supplemental figure 3). Four out of 105 tested proteins showed a significant correlation (figure 6a-d). Higher levels of the chemokine stromal cell derived factor-1 alpha (SDF-1a) correlated with higher histological score ($r = 0.58$ $p = 0.038$). The three proteins with a negative regression coefficient with right injury score are involved in the regulation of the inflammatory response: interleukin-1 receptor antagonist (IL-1Ra: $r = -0.65$ $p = 0.023$), interleukin-5 (IL-5: $r = -0.61$ $p = 0.027$) and granulocyte-macrophages colony-stimulating factor (GM-CSF: $r = -0.64$ $p = 0.018$).

Interestingly, right lung injury score was not correlated with circulating levels of LPS ($r = 0.12$ $p = 0.659$) (Supplemental Figure 4).

Systemic inflammation, drive and effort. Our experimental study showed that respiratory effort and drive are directly correlated with systemic inflammation. Both ΔP_{es} and ΔP_L were correlated with IGFBP-3 ($r = 0.66$ $p = 0.019$ and $r = 0.69$ $p = 0.009$), TNF-alpha ($r = 0.68$ $p = 0.011$ and $r = 0.6$ $p = 0.015$), IL-13 ($r = 0.59$ $p = 0.033$ and $r = 0.62$ $p = 0.023$) and IL-1beta ($r = 0.68$ $p = 0.011$ and $r = 0.64$ $p = 0.019$) (Figure 7a-d), while P0.1 was correlated with IL-31 ($r = 0.71$ $p = 0.007$) (figure 7e).

Discussion

The main findings of this experimental study on an animal model of bilateral lung injury initiated by a pro-inflammatory insult to a single lobe are: a) despite standardized methods to induce the primary left lobar insult, severity of right lung injury varies widely among animals; b) development of injury in previously healthy right lung results from specific pathophysiological mechanisms related to increased respiratory drive and effort; c) explorative proteomic analysis suggests specific biomarkers with injurious and/or protective effects for right lung injury, and highlights the effects of systemic inflammation on increased respiratory drive and effort.

Pneumonia is the leading cause of ARDS in clinical studies (22). Our experimental model replicated the pathophysiological combination of localized pulmonary inflammation and increased drive and effort which likely characterizes the progression from pneumonia to ARDS. On the other hand, it presumably represents just a simplified explorative approach, as other important factors like different etiologic agents, primary lobe involved, insult intensity, patient characteristics, etc. still need to be properly addressed.

Inter-individual variability of right lung injury score occurring in this standardized animal model could suggest a role for genetic factors which modulate the response to the initial pro-inflammatory stimulus in many ways (23). Activation of lung inflammation, due for example to cytokines genes variations, could affect the progression to bilateral injury, both directly and through increased respiratory drive and effort (24)(25). Genetic variations could have also led to more intense respiratory effort for the same inflammatory activation. Indeed, genetic polymorphisms linked to inflammatory pathways may alter both the susceptibility to ARDS and severity (26).

We observed correlations between right lung injury and increased drive and effort, as assessed by $P_{0.1}$, ΔP_{es} and ΔP_{occ} , and with the downstream increase in lung stress. This has important consequences on the monitoring of spontaneously breathing patients with pneumonia at risk of progression to ARDS.

Surprisingly, not all the consequences of increased drive and effort resulted relevant for right lung injury. As far as ventilatory pattern is concerned, we found that larger V_t did not correlate with the right histological score. Tidal volume is considered a surrogate target for lung protection in the clinical management of spontaneously breathing ARDS patients undergoing non-invasive ventilation (11). However, V_t does not constantly and predictably reflect respiratory effort because of the interaction with lung compliance and heterogeneous distribution of ventilation. At variance, tidal strain, measuring the increase of lung volume normalized by starting inflation, correlated well with right injury score in our model of initially localized pulmonary insult. Monitoring of more specific variables such as driving pressure and strain could increase our ability to protect the lungs.

The correlation between respiratory rate and severity of right lung injury suggests that activation of respiratory drive resulted in tachypnea in this animal model; more importantly, it supported the role of respiratory rate (and thus of mechanical power) in the progression to bilateral lung injury (27). Pressure-time product, indeed, is a metabolic measurement of respiratory work which incorporates per breath effort and respiratory rate (28) and was correlated with right lung injury score, potentially suggesting its role as monitor of lung protection.

Our data confirm the hypothesis that negative (sub-atmospheric) values of P_{alv} during inspiration contribute to progression to bilateral injury (29). This, and the protective role of positive transpulmonary pressure at end-expiration, also confirm that use of higher PEEP

could be protective, by attenuating capillary leak, preventing cyclic alveolar collapse and/or limiting diaphragm efficiency (5).

The explorative proteomic analysis identified biomarkers with physiologically sound correlations with right lung injury severity. For example, the positive correlation between SDF-1 and histological score is supported by the role of this chemokine in the sustained recruitment of neutrophils involved in the progression of lung injury in murine models (30). Among the three “protective” biomarkers negatively correlated with right lung injury score, IL-1Ra and IL-5 protect against the adverse effects of excessive inflammatory response. Indeed, an experimental study showed that IL-1Ra modulates the susceptibility to LPS-induced lung injury in mice (31). As for GM-CSF, this mediator could limit early epithelial cell injury and maintain alveolar macrophage function in the lung (32, 33). Blockade of injurious biomarkers, like SDF-1, or administration of protective factors, like GM-CSF, represent fascinating pharmacological perspectives to modulate progression to bilateral injury, or even to prevent it. Early use might be key to their efficacy, as some of these approaches failed to improve clinical outcome in patients with established ARDS (34). Regulation of inflammatory response might also allow effective control of respiratory drive and effort. Stimulation of brain respiratory centers could possibly occur in two ways: systemic release of inflammatory mediators from the insulted lobe and/or neural signaling from the inflamed lung via the vagus nerve (35). Plasmatic levels of inflammatory cytokines were correlated with ΔP_{es} and ΔP_{L} in our model; while, at variance from observations in patients, we could not find a correlation between most inflammatory cytokines and $P_{0.1}$, except IL-31. Overall, these data suggest that lung inflammation is associated with increased respiratory drive and effort.

Our study has many limitations. First, generalizability of this model of localized lung injury could be questioned since lobar inflammation by LPS could differ from bacterial, viral or

aspiration pneumonia, in terms of intensity, evolution, systemic reaction. Second, right lung injury was quantified by histological score at the end, while in-vivo assessment along the experiment might improve our understanding on how and when lobar inflammation starts affecting surrounding lung regions and improve human translation. Third, proteomic analysis was performed with commercially available human kits: while the consistent signal suggest that results are reliable, specific reporting standards are lacking. Finally, correlation does not imply causation: conclusive evidence demonstrating whether increased drive and effort are determinants of injury, consequences of injury, or both, is still lacking.

In conclusion, we developed a novel experimental model of bilateral lung injury from localized lobar inflammation induced by LPS: this resulted in increased respiratory drive and effort and in the development of contralateral lung damage within 24 hours, albeit with significant inter-animal variability. We described specific pathophysiological mechanisms associated with progression to right lung injury, deriving from increased respiratory effort, which stands out as principal responsible for the injury and as target parameter for early monitoring. The explorative proteomic analysis suggests candidate pathways of inflammatory response, whose modulation could potentially prevent progression to bilateral injury.

References:

1. Brochard L, Slutsky A, Pesenti A. Mechanical Ventilation to Minimize Progression of Lung Injury in Acute Respiratory Failure. *Am J Respir Crit Care Med* 2017;195:438–442.
2. Yoshida T, Uchiyama A, Matsuura N, Mashimo T, Fujino Y. Spontaneous breathing during lung-protective ventilation in an experimental acute lung injury model. *Crit Care Med* 2012;40:.
3. Yoshida T, Uchiyama A, Matsuura N, Mashimo T, Fujino Y. The comparison of spontaneous breathing and muscle paralysis in two different severities of experimental lung injury. *Crit Care Med* 2013;41:.
4. Yoshida T, Torsani V, Gomes S, Santis RRD, Beraldo MA, Costa ELV, *et al.* Spontaneous effort causes occult pendelluft during mechanical ventilation. *Am J Respir Crit Care Med* 2013;188:.
5. Morais CCA, Koyama Y, Yoshida T, Plens GM, Gomes S, Lima CAS, *et al.* High positive end-Expiratory pressure renders spontaneous effort noninjurious. *Am J Respir Crit Care Med* 2018;197:.
6. Cai Z, Zhang H, Guo X, Song L. Resistive spontaneous breathing exacerbated lipopolysaccharide-induced lung injury in mice. *Biochem Biophys Res* 2024;38:101726.
7. Slobod D, Assanangkornchai N, Samoukovic G. Getting SILI between Two Extracorporeal Membrane Oxygenation Runs. *Ann Am Thorac Soc* 2021;.
8. Le Marec J, Hajage D, Decavèle M, Schmidt M, Laurent I, Ricard J-D, *et al.* High Airway Occlusion Pressure Is Associated with Dyspnea and Increased Mortality in Critically Ill Mechanically Ventilated Patients. *Am J Respir Crit Care Med* 2024;210:.
9. Coppola S, Chiumello D, Busana M, Giola E, Palermo P, Pozzi T, *et al.* Role of total lung stress on the progression of early COVID-19 pneumonia. *Intensive Care Med* 2021;47:.
10. Tonelli R, Fantini R, Tabbì L, Castaniere I, Pisani L, Pellegrino MR, *et al.* Early inspiratory effort assessment by esophageal manometry predicts noninvasive ventilation outcome in de novo respiratory failure: A pilot study. *Am J Respir Crit Care Med* 2020;202:.
11. Carteaux G, Millán-Guilarte T, De Prost N, Razazi K, Abid S, Thille AW, *et al.* Failure of Noninvasive Ventilation for de Novo Acute Hypoxemic Respiratory Failure: Role of Tidal Volume*. *Crit Care Med* 2016;44:.
12. Bachmann MC, Cruces P, Díaz F, Oviedo V, Goich M, Fuenzalida J, *et al.* Spontaneous breathing promotes lung injury in an experimental model of alveolar collapse. *Sci Rep* 2022;12:.
13. Bellani G, Laffey JG, Pham T, Madotto F, Fan E, Brochard L, *et al.* Noninvasive Ventilation of Patients with Acute Respiratory Distress Syndrome: Insights from the LUNG SAFE Study. *Am J Respir Crit Care Med* 2017;195:.
14. Mascheroni D, Kolobow T, Fumagalli R, Moretti MP, Chen V, Buckhold D. Acute respiratory failure following pharmacologically induced hyperventilation: an experimental animal study. *Intensive Care Med* 1988;15:.
15. Frat J-P, Thille AW, Mercat A, Girault C, Ragot S, Boulain T, *et al.* High-Flow Oxygen through Nasal Cannula in Acute Hypoxemic Respiratory Failure. *n engl j med* 2015;23:2185–96.
16. Marongiu I, Spinelli E, Scotti E, Mazzucco A, Wang Y-M, Manesso L, *et al.* Addition of 5% CO₂ to Inspiratory Gas Prevents Lung Injury in an

- Experimental Model of Pulmonary Artery Ligation. *Am J Respir Crit Care Med* 2021;204:933–942.
17. Bertoni M, Telias I, Urner M, Long M, Del Sorbo L, Fan E, *et al.* A novel non-invasive method to detect excessively high respiratory effort and dynamic transpulmonary driving pressure during mechanical ventilation. *Crit Care* 2019;23:.
 18. Franchineau G, Jonkman AH, Piquilloud L, Yoshida T, Costa E, Rozé H, *et al.* Electrical Impedance Tomography to Monitor Hypoxemic Respiratory Failure. *Am J Respir Crit Care Med* 2023;doi:10.1164/rccm.202306-1118CI.
 19. Menga LS, Cese LD, Rosà T, Cesarano M, Scarascia R, Michi T, *et al.* Respective Effects of Helmet Pressure Support, Continuous Positive Airway Pressure, and Nasal High-Flow in Hypoxemic Respiratory Failure A Randomized Crossover Clinical Trial. *Am J Respir Crit Care Med* 2023;207:1310–1323.
 20. Cornejo RA, Arellano DH, Ruiz-Rudolph P, Guíñez D V, Morais CCA, Gajardo AIJ, *et al.* Inflammatory biomarkers and pendelluft magnitude in ards patients transitioning from controlled to partial support ventilation. *Sci Rep* 2022;12:20233.
 21. Bellani G, Laffey JG, Pham T, Fan E, Brochard L, Esteban A, *et al.* Epidemiology, patterns of care, and mortality for patients with acute respiratory distress syndrome in intensive care units in 50 countries. *JAMA - Journal of the American Medical Association* 2016;315:.
 22. WATERER GW, QUASNEY MW, CANTOR RM, WUNDERINK RG. Septic Shock and Respiratory Failure in Community-acquired Pneumonia Have Different TNF Polymorphism Associations. *Am J Respir Crit Care Med* 2001;163:1599–1604.
 23. Baedorf-Kassis E, Murn M, Dzierba AL, Serra AL, Garcia I, Minus E, *et al.* Respiratory drive heterogeneity associated with systemic inflammation and vascular permeability in acute respiratory distress syndrome. *Crit Care* 2024;28:136.
 24. Ma P, Chen D, Pan J, Du B. Genomic polymorphism within interleukin-1 family cytokines influences the outcome of septic patients*. *Crit Care Med* 2002;30:1046–1050.
 25. Marshall RP, Webb S, Hill MR, Humphries SE, Laurent GJ. Genetic Polymorphisms Associated With Susceptibility and Outcome in ARDS. *Chest* 2002;121:68S-69S.
 26. Protti A, Maraffi T, Milesi M, Votta E, Santini A, Pugini P, *et al.* Role of Strain Rate in the Pathogenesis of Ventilator-Induced Lung Edema*. *Crit Care Med* 2016;44:e838–e845.
 27. Sassoon CSH, Light RW, Lodia R, Sieck GC, Mahutte CK. Pressure-time product during continuous positive airway pressure, pressure support ventilation, and T-piece during weaning from mechanical ventilation. *American Review of Respiratory Disease* 1991;143:.
 28. Bellani G, Grasselli G, Teggia-Droghi M, Mauri T, Coppadoro A, Brochard L, *et al.* Do spontaneous and mechanical breathing have similar effects on average transpulmonary and alveolar pressure? A clinical crossover study. *Crit Care* 2016;20:.
 29. Petty JM, Sueblinvong V, Lenox CC, Jones CC, Cosgrove GP, Cool CD, *et al.* Pulmonary Stromal-Derived Factor-1 Expression and Effect on Neutrophil

- Recruitment during Acute Lung Injury. *The Journal of Immunology* 2007;178:8148–8157.
30. Hirsch E, Irikura VM, Paul SM, Hirsh D. Functions of interleukin 1 receptor antagonist in gene knockout and overproducing mice. *Proceedings of the National Academy of Sciences* 1996;93:11008–11013.
 31. Paine R, Wilcoxon SE, Morris SB, Sartori C, Baleeiro CEO, Matthay MA, *et al.* Transgenic Overexpression of Granulocyte Macrophage-Colony Stimulating Factor in the Lung Prevents Hyperoxic Lung Injury. *Am J Pathol* 2003;163:2397–2406.
 32. Matute-Bello G, Liles CW, Radella F, Steinberg KP, Ruzinski JT, Hudson LD, *et al.* Modulation of neutrophil apoptosis by granulocyte colony-stimulating factor and granulocyte/macrophage colony-stimulating factor during the course of acute respiratory distress syndrome. *Crit Care Med* 2000;28:1–7.
 33. Paine R, Standiford TJ, Dechert RE, Moss M, Martin GS, Rosenberg AL, *et al.* A randomized trial of recombinant human granulocyte-macrophage colony stimulating factor for patients with acute lung injury*. *Crit Care Med* 2012;40:90–97.
 34. Jacono FJ, Mayer CA, Hsieh Y-H, Wilson CG, Dick TE. Lung and brainstem cytokine levels are associated with breathing pattern changes in a rodent model of acute lung injury. *Respir Physiol Neurobiol* 2011;178:429–438.

ARTICLE IN PRESS

Figure legends

Figure 1. Distribution of the severity of right lung injury. The figure shows the distribution of right lung injury score in both LPS and Sham animals. The score was in the lower ranges in Sham animals, while it was normally distributed across a wide interval in LPS group, indicating inter-individual variability. * $p < 0.05$ SHAM vs. LPS

Figure 2. Representative images for histology, immunohistochemistry and strain by EIT in animals with different right lung injury severity, compared to Sham. Animals with a right lung histological score > 10 (A) showed significant thickening of the alveolar walls and alveolar lining cell injury, culminating in complete pulmonary hepatization, with fluids exudate containing immune cells, red blood cells and fibrin. Animals with a right histological score ≤ 10 (b) revealed some loss of alveolar integrity, haemorrhage and granulocyte infiltration. The alveolar wall with a single layer of alveolar epithelial cells was preserved in sham animals (c).

Immunohistochemistry for ionized calcium-binding adapter molecule-1 (IBA-1) showed clusters of macrophages (stained in brown), diffuse within the lung parenchyma of LPS animals with more severe right lung injury (d), while macrophages are distributed in the alveolar wall, but at a lower density in milder cases (e). Few resident macrophages are present in sham animals (f).

EIT-derived strain, measuring tidal deformation indicized by the starting lung unit volume, showed progressively higher intensity in sham, mild and more severe right lung injury (g-i).

Figure 3. Correlations between right lung injury score and respiratory pattern. Higher histological score is correlated with higher respiratory rate, minute ventilation and pressure-time product, but not with tidal volume.

Figure 4. Correlations between right lung histological score and respiratory drive and effort. The score is correlated with $P_{0.1}$, ΔP_{es} and ΔP_{occ}

Figure 5. Correlations between right lung histological score and stress, strain and pendelluft. Maximal stress (dynamic inspiratory transpulmonary pressure), tidal stress (transpulmonary driving pressure) and tidal strain (EIT-derived), but not occult pendelluft, are correlated with the histological right lung score.

Figure 6. Correlations between systemic inflammation and injury. Significant correlation with higher histological scores was disclosed for stromal cell derived factor-1 alfa (SDF-1a), thus indicating a possible role in the worsening of acute lung damage. Conversely, interleukin-1 receptor antagonist (IL-1Ra), interleukin-5 (IL-5), granulocyte-macrophages colony-stimulating factor (GM-CSF) showed a negative correlation, suggesting a possible protective effect.

Figure 7. Correlations between systemic inflammation and respiratory effort and drive
A positive correlation was found between ΔP_{es} and four inflammatory proteins: Insulin-like Growth Factor Binding Protein 3 (IGFBP-3), IL-1beta, IL-13 and TNF-alfa (Figure 7 a-d), while P0.1 was correlated with IL-31 (7 e).

Table 1. Physiological differences between LPS and Sham groups

	Sham (n=5)	LPS (n=18)	P-value
Histological score			
Global	11 [6-16]	37 [31-44]	0.003
Left lung	6 [3-9]	27 [22-31]	0.001
Right lung (SILI score)	6 [3-9]	10.5 [8-14]	0.045
Gas exchanges			
PaO ₂ /FiO ₂ (mmHg)	454 [336—488]	361 [326- 398]	0.061
Ventilatory ratio	1.6 [1.2-1.9]	2.2 [1.8-2.7]	0.013
PaCO ₂ (mmHg)	49 [46-54]	39 [36-44]	0.007
pH	7.43 [7.42-7.44]	7.48 [7.45-7.50]	0.004
Ventilation, drive and effort			
MV (L/min)	3.7 [2.6-5.3]	7.6 [6-9.6]	0.032
Vt (ml/kg)	5.4 [4.5-6.4]	5.9 [4.7-8]	0.480
ΔP _L (cmH ₂ O)	7.2 [6.0-8.3]	12.4 [9.4-15.7]	0.004
ΔPes (cmH ₂ O)	2.96 [1.54-3.64]	8.1 [4.9-10.8]	0.004
RR (bpm)	21 [13-28]	31 [27-47]	0.025
P0.1 (cmH ₂ O)	0.95 [1.39-1.49]	3.5 [1.99-5.32]	0.004
Sedation			
Propofol (mg/kg/h)	128 [86-131]	104 [88-122]	0.434
Hemodynamics			
SAP (mmHg)	97 [95-102]	104 [96-121]	0.260
MAP (mmHg)	77 [74-85]	79 [73-94]	0.650
DAP (mmHg)	56 [53-66]	62 [51-77]	0.460
Heart rate (bpm)	76 [76-92]	107 [98-116]	0.003
PAPs (mmHg)	23 [23-25]	23 [19-24]	0.240
PAPm (mmHg)	18 [16-19]	18 [14-20]	0.620
PAPd (mmHg)	12 [10-14]	10 [7-15]	0.450
PCWP (mmHg)	6 [5-7]	8 [7-12]	0.031
Cardiac Output (L/min)	3.4 [3.4-4.1]	4.2 [3.9-4.5]	0.060
Fluid Balance at T 24 (ml)	315 [259-446]	303 [200-620]	0.910
Arterial Lactates (mmol/l)	0.7 [0.7-1.1]	0.7 [0.7-1.1]	0.940

Abbreviations: PaO₂: arterial oxygen partial pressure; PaCO₂: arterial carbon dioxide partial pressure; MV: minute ventilation; RR: respiratory rate, Vt: tidal volume; ΔP_L: transpulmonary driving pressure; ΔPes: esophageal pressure swing; P0.1: airway occlusion pressure; SAP: systolic arterial pressure; MAP: mean arterial pressure; DAP: diastolic arterial pressure; PAPs/m/d: pulmonary arterial pressure systolic/mean/diastolic; PCWP: pulmonary capillary wedge pressure

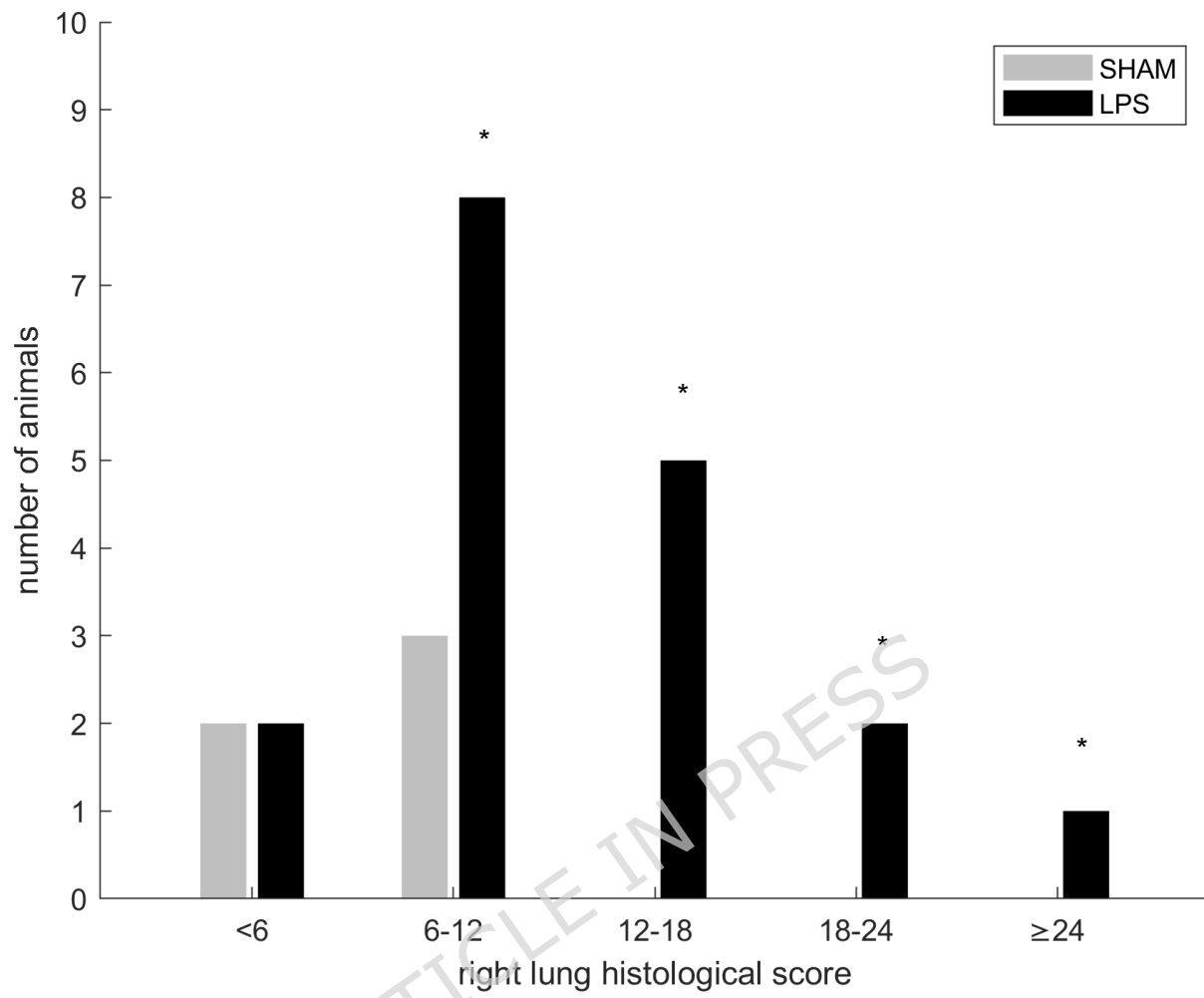
Figure 1.

Figure 2.

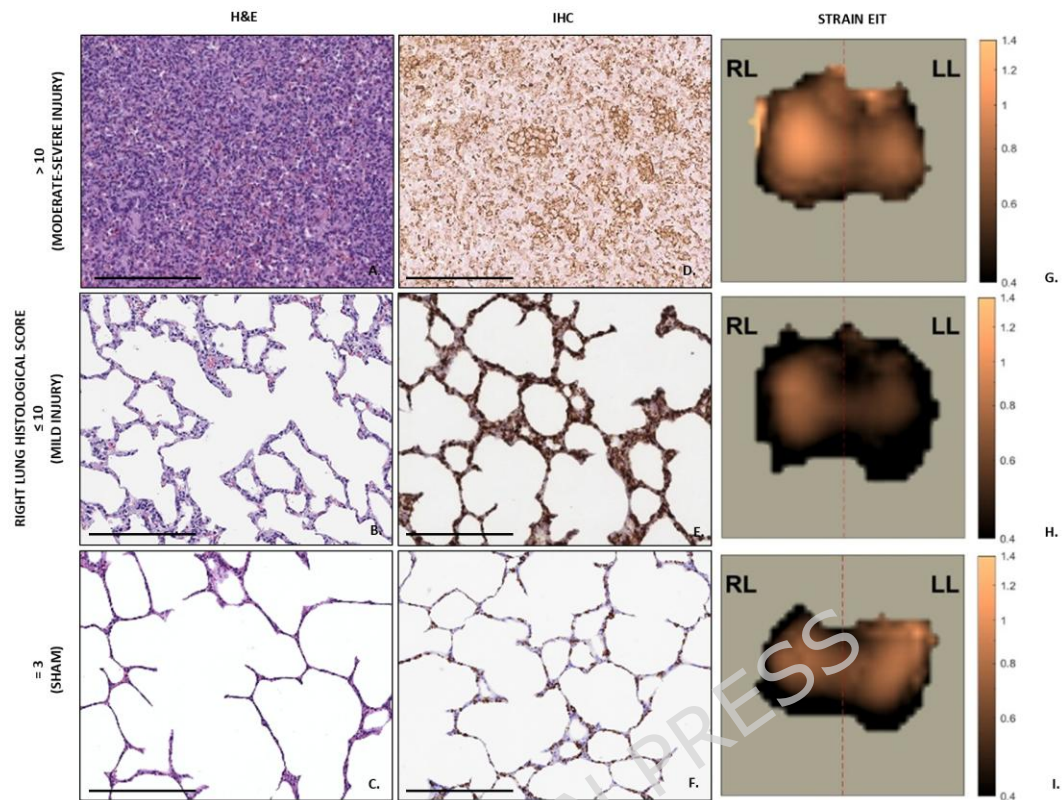


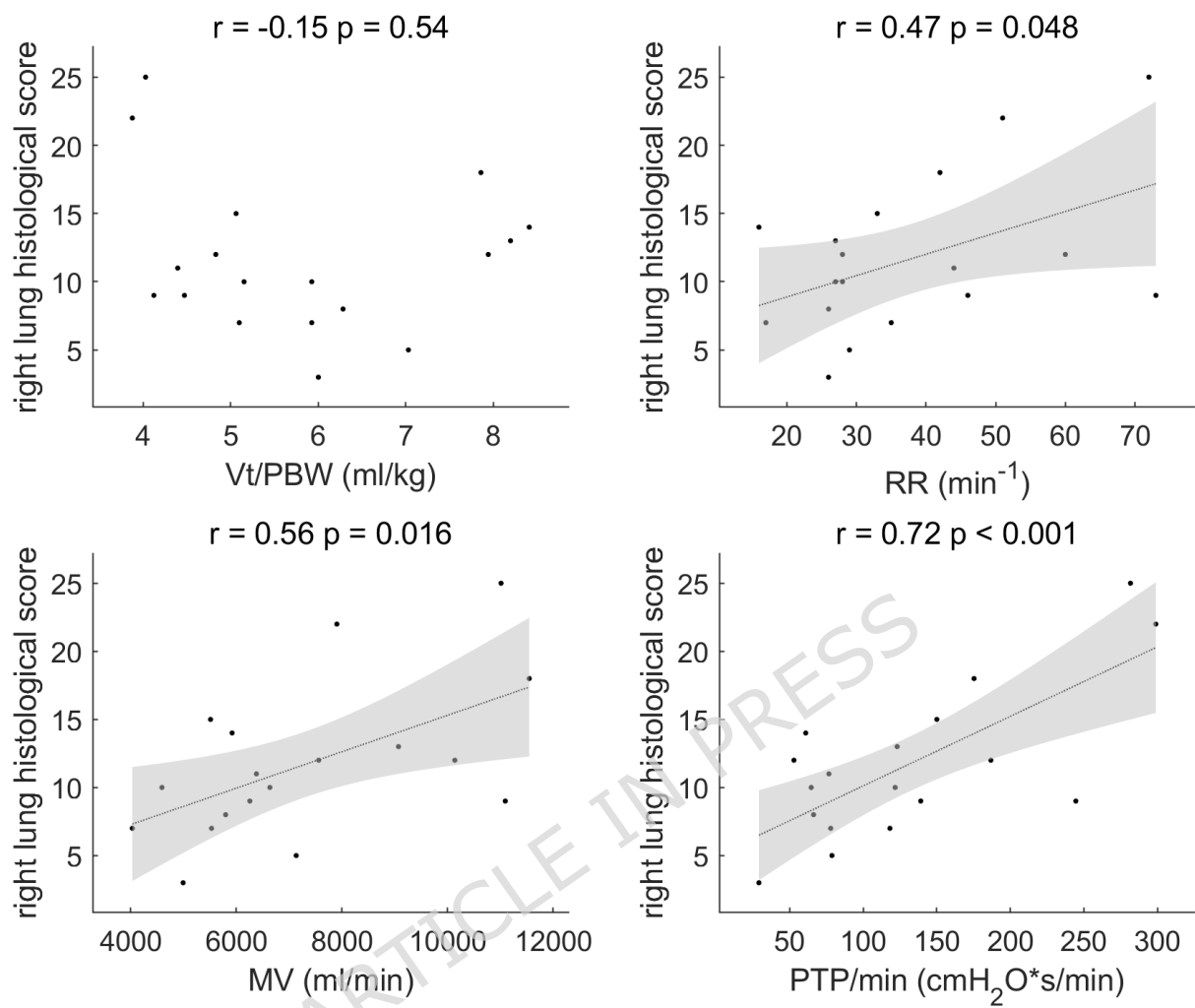
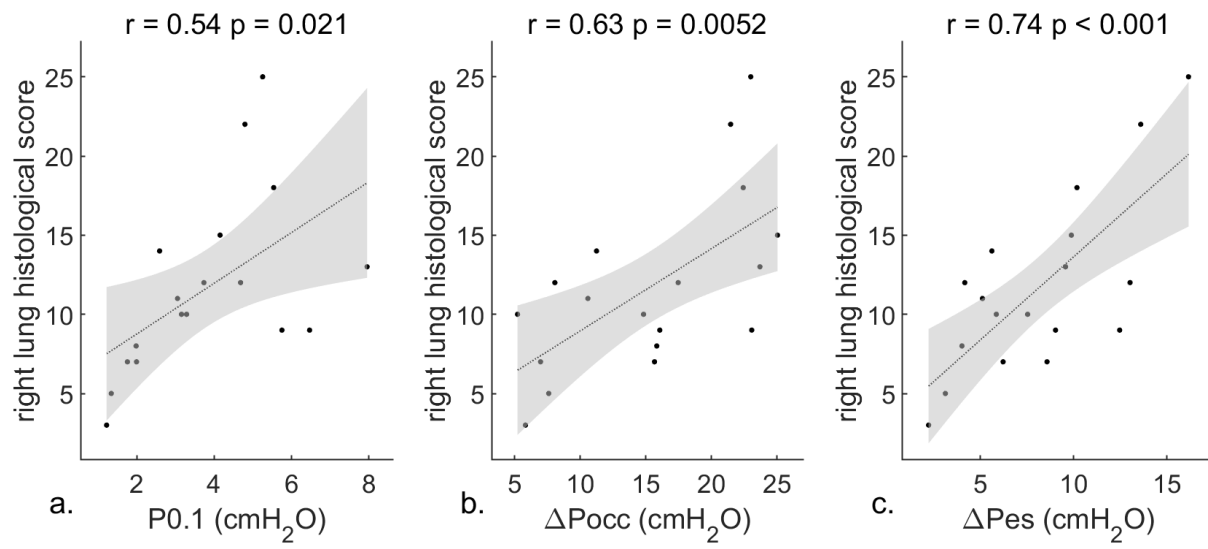
Figure 3.

Figure 4.

ARTICLE IN PRESS

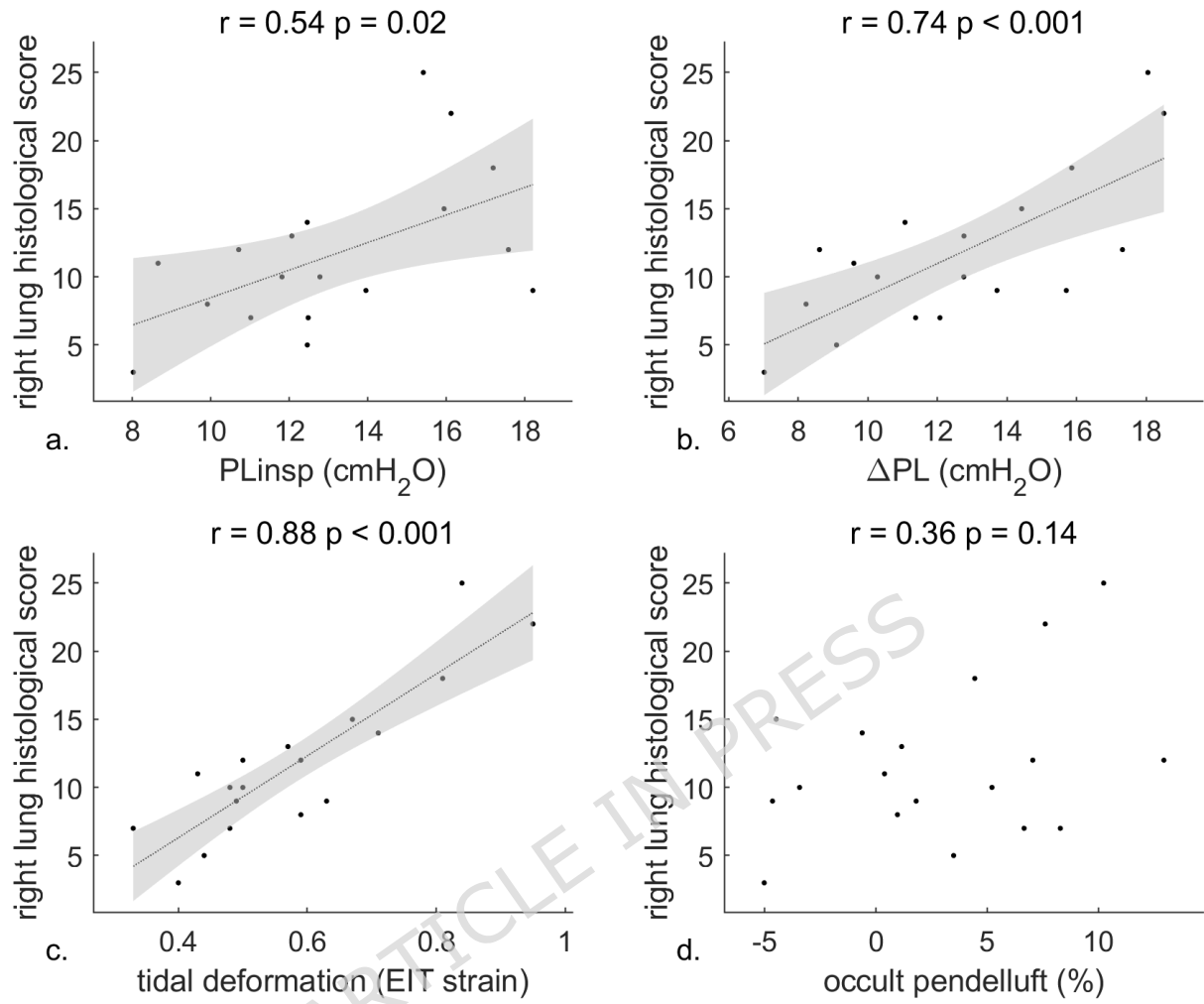
Figure 5.

Figure 6.

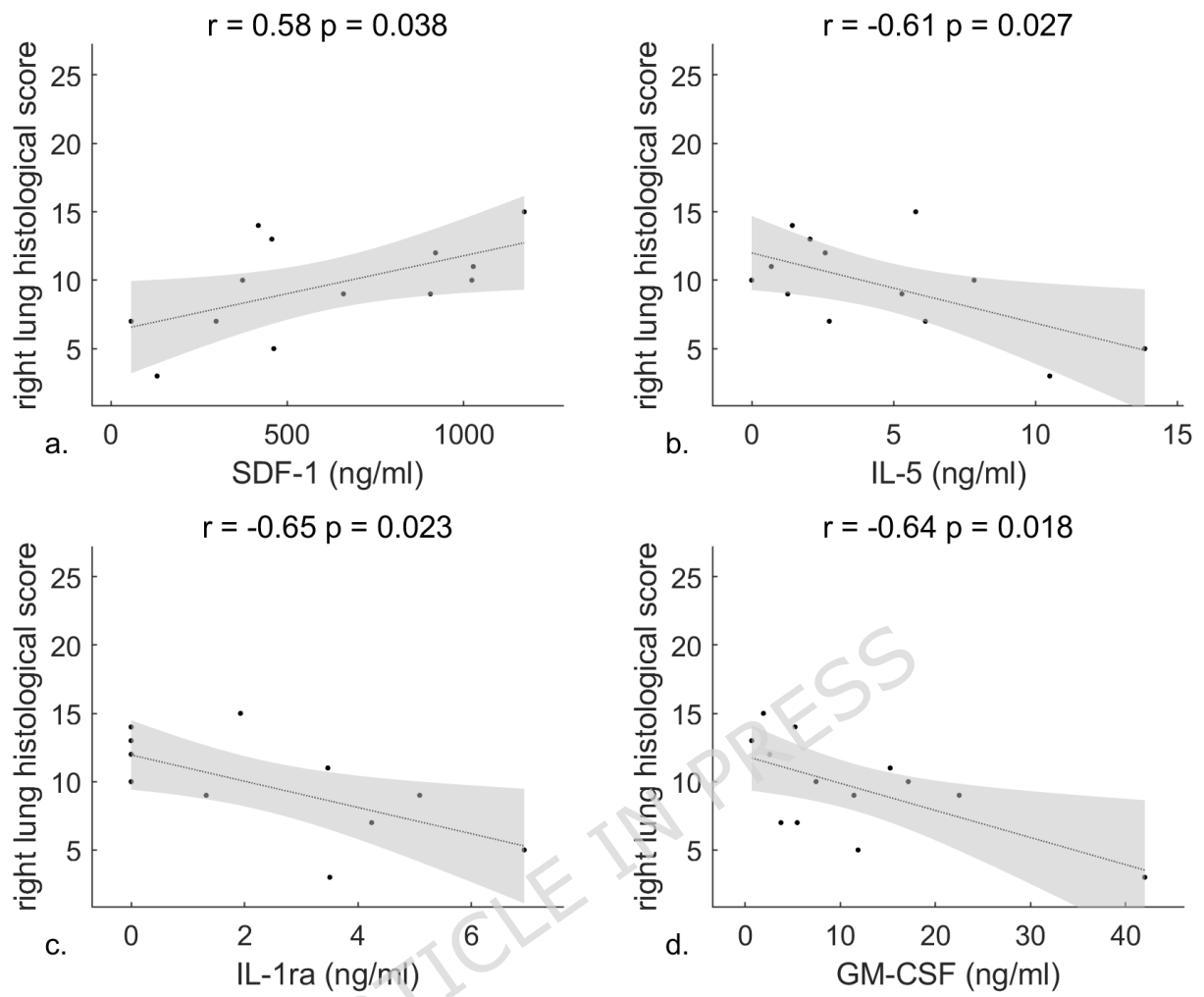
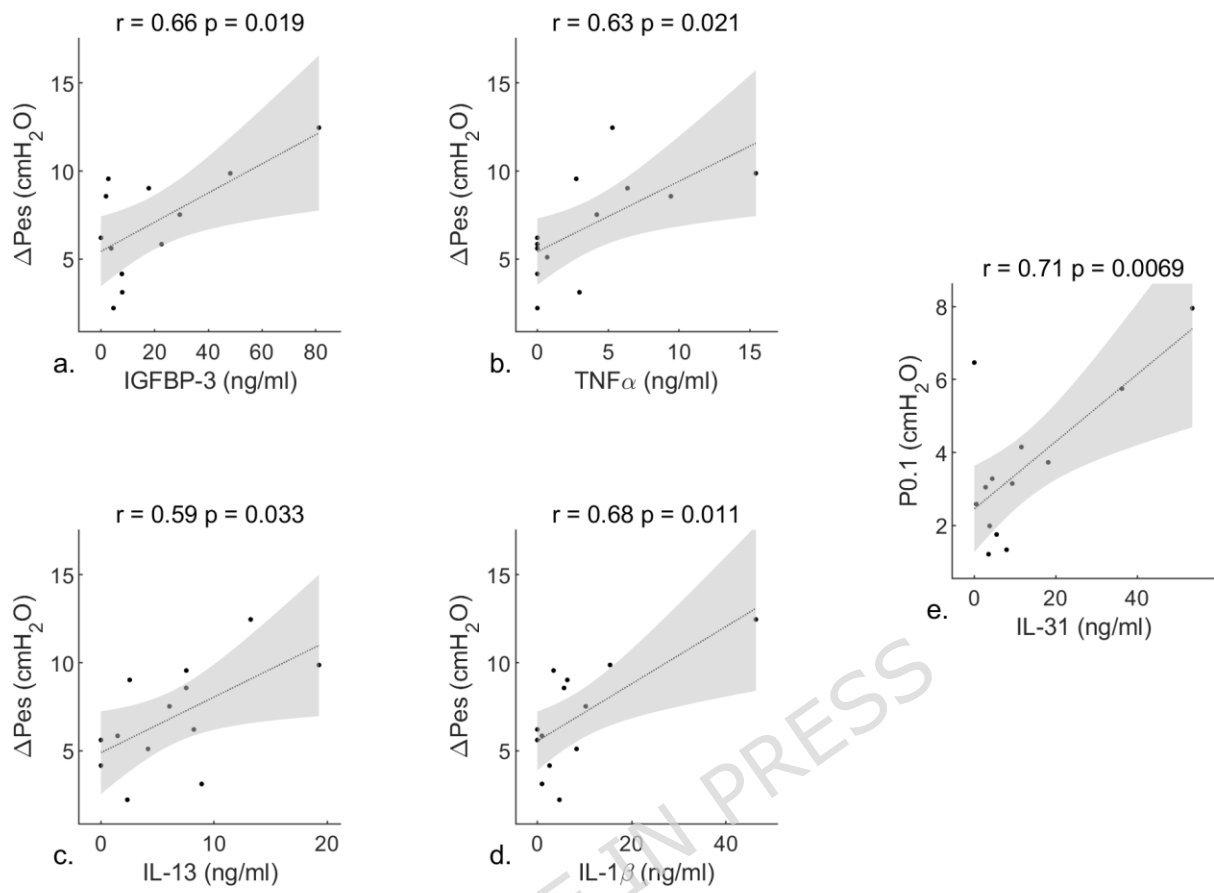


Figure 7.

Declarations:

Ethics approval: the study protocol was approved by the Italian Ministry of Health, Rome, Italy (Ref. n° 855/2024-PR prot. 568EB.49)

Consent for publication: not applicable

Availability of data and materials: The datasets used and/or analysed during the current study are available from the corresponding author on reasonable request.

Competing interests: TM, personal fees for speaking at sponsored symposia by Draeger, Fisher and Paykel, Aerogen, outside of the submitted work. GG, personal fees from Getinge, Draeger, Fisher & Paykel (payment for lectures), outside of the submitted work. All other authors, none.

Funding: Institutional funding of the Department of Anesthesia, Critical Care and Emergency, Fondazione IRCCS Ca' Granda Ospedale Maggiore Policlinico, Milan, Italy; Current research, Italian Ministry of Health, Rome, Italy; Project "Hub Life Science - Diagnostica Avanzata (HLS-DA), PNC-E3-2022-23683266– CUP: C43C22001630001 / MI-0117", Italian Ministry of Health, Rome, Italy (Piano Nazionale Complementare Ecosistema Innovativo della Salute); The Italian Ministry of Education and Research (MUR), Rome Italy: Dipartimenti di Eccellenza Program 2023–2027 - Dept. of Pathophysiology and Transplantation, University of Milan.

Author's contributions to the study: Substantial contributions to the conception or design of the work: TM, ES. Acquisition, analysis, or interpretation of data for the work: TM, ES, IM, AD, ML, AM, LC, FD, GL, AZ, LR, VV, GG. Drafting the work or revising it critically for important intellectual content: TM, ES, IM, AD, ML, AM, LC, FD, GL, AZ, LR, VV, GG. Final approval of the version submitted for publication: TM, ES, IM, AD, ML, AM, LC, FD, GL, AZ, LR, VV, GG. Accountability for all aspects of the work in ensuring that questions related to the accuracy or integrity of any part of the work are appropriately investigated and resolved: TM, ES, IM, AD, ML, AM, LC, FD, GL, AZ, LR, VV, GG.

Acknowledgements: The authors wish to thank all the personnel from the laboratory of preclinical research of the Maggiore Policlinico Hospital, Milan, Italy, for their support.

Additional material: Additional study details can be found in the online Supplement

ARTICLE IN PRESS